Proceedings of the 1999 IEEE
International Conference on Robotics & Automation
Detroit, Michigan • May 1999

An Independent Joint-Based Compliance Control Method for a Five-bar Finger Mechanism Via Redundant Actuators.

B.R. So[1], B.-J. Yi[1], S.-R. Oh[2], I.H. Suh[1]

[1]Dept. of Electrical Eng. and Computer Science, Hanyang Univ. Korea
[2]Intelligent System Control Research Center, KIST, Korea
bj@email.hanyang.ac.kr

Abstract

In this paper, we discuss an inherent problem occurring in former operational-based compliance control scheme. In order to obviate this problem, an independent joint-based compliance control scheme is proposed. This control method requires that for the adjustment of the operational compliance matrix, a manipulator should have at least the same number of joints as the number of independent components of the desired compliance matrix specified in the operational space. Types of robot structures which are appropriate to independent joint-based compliance scheme are addressed. A five-bar finger with redundant actuators is treated as an illustrative example. Our experimental results show that former compliance control schemes does not guarantee modulation of the required operational compliance matrix, while performance of the proposed compliance modulation method has been satisfactory. We also consider an additional stiffness effect due to the antagonistic fighting between the controlled-operational force and the equilibriumed joint torque vector. It is also experimentally shown that consideration of this additional term notably improves the force tracking performance of the given mechanism.

1. Introduction

The Human body, general mammals, and insects possess redundant actuators in their musculoskeltal structures. Redundant actuation implies that there exists more actuators than the system's degree-of-freedom. Recently, applications of redundant actuation to robotics have been an active research field. Multiple arms, multi-fingered hands, and walking machine are included as such examples[1-4, 18-21]. In this work, we present a compliant control method which beneficially utilizes the advantage of redundant actuation.

Salisbury [6] presented a compliance control scheme in the operational space. Once compliance matrix (or stiffness matrix $[K_{uu}]$) is designed, the joint space compliance matrix(or stiffness matrix $[K_{\phi\phi}]$) is obtained as

$$[K_{\phi\phi}] = [G_{\phi}^{u}]^{T}[K_{uu}][G_{\phi}^{u}], \qquad (1)$$

where $[G_{\phi}^{u}]$ denotes the Jacobian relating the output to the input. Compliance control capability is an important feature for robot interacting with environment or another robot.[5-10] Based on this principle, recently many compliance control algorithms have been reported in the field of redundant manipulators [11-13] and multiple arms [12] holding a common object. Different from the former methods, joint-based compliance schemes have been reported. Mussa-Ivaldi and Hogan [11] proposed a joint-based compliance scheme to redundant manipulators. However, the method has not discussed how to modulate a desired operational compliance. Tanie, et.al. also proposed a joint-base compliance scheme [12]. The so called *Direct Compliance Control* uniquely determines the manipulator configuration. This control method requires that for the adjustment of the operational compliance matrix, a manipulator should have at least the same number of joints as the number of independent components of the desired compliance matrix specified in the operational space. However, they considered only the case of kinematically redundant manipulators. Accordingly, the number of joints increases as many as the number of degrees of the operational space. Thus, the resulting configuration may not be appropriate in the design viewpoint. They also proposed a combined compliance control method [13] of a redundant manipulator. It was constructed by combining two different compliance control schemes ; Initially they define a diagonal joint compliance matrix which is arbitrarily decided and transforms it to an effective operational stiffness matrix. Secondly, the offset stiffness matrix is calculated as the difference between the desired operational stiffness matrix and the effective stiffness matrix. Then, by employing the usual stiffness mapping of Eq. (1), a joint compliance matrix is obtained. Their experimental result was satisfactory.

In this paper, we consider a joint-based compliance control scheme. Especially, we explain, in our point of view, why the former operational-based compliance control scheme is not appropriate, which naturally introduces the necessity of independent joint-based compliance control scheme. Also, we propose types of robot structures which

0-7803-5180-0-5/99 $10.00 © 1999 IEEE

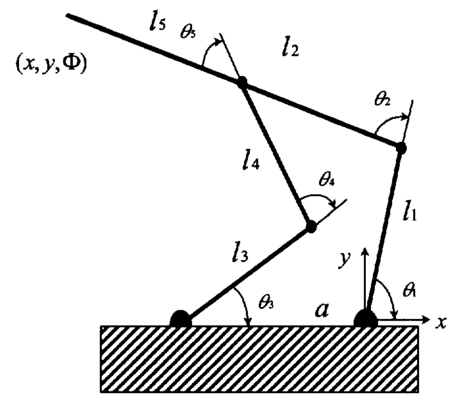

Fig. 1 : Five-bar Finger Mechanism

are much appropriate to independent joint-based compliance scheme. These structures are anthropomorphic, and possess force redundancy as well as kinematic redundancy, which enables us to modulate the operational stiffness in a more adequate way. As an illustrative example, we investigate a five-bar finger mechanism (Fig. 1) which has two redundant actuators in its structure. Our experimental results show that former compliance control schemes does not always guarantee modulation of the required operational compliance matrix, while the compliance modulation of the proposed method will be satisfactory. We also consider an additional stiffness effect due to the antagonistic fighting between the controlled-operational force and the equilibriumed joint torque vector. It is experimentally shown that consideration of this additional term notably improves the force tracking performance of the given mechanism.

2. *Independent Joint-Based Compliance Control Scheme*

In the former operational-based compliance control scheme, the effective joint-space stiffness matrix is defined in the following equation [6] :

$$\boldsymbol{\tau} = [K_{\phi\phi}]\Delta\boldsymbol{\phi} = [K_{\phi\phi}][G_u^{\phi}]\Delta\boldsymbol{u}, \qquad (2)$$

where $\Delta\boldsymbol{u}$ and $\Delta\boldsymbol{\phi}$ denote the differential change of the displacement in the operational space and the joint space, respectively. And, $[G_u^{\phi}]$ denotes the inverse of $[G_{\phi}^{u}]$. Substituting Eq. (1) into Eq. (2) yields

$$\boldsymbol{\tau} = [G_{\phi}^{u}]^T[K_{uu}]\Delta\boldsymbol{u} \qquad (3)$$

and rearranging it at the implicit relationship between $\boldsymbol{\tau}$ and $\boldsymbol{k_u}$ given by

$$\boldsymbol{\tau} = [A]\,\boldsymbol{k_u}, \qquad (4)$$

where the matrix $[A]$ is the function of joint angles and $\Delta\boldsymbol{u}$, and the vector $\boldsymbol{k_u}$ consists of the independent stiffness elements of the operational space stiffness matrix. Let N denote the degree-of-freedom in the operational space. Then, the dimensions of $\boldsymbol{k_u}$, $\boldsymbol{\tau}$, and $[A]$ will be $N(N+1)/2$, N for serial manipulator, and $N\times N(N+1)/2$, respectively. For example, consider a five-bar mechanism shown in Fig. 1 which has two degree-of-freedom in the operational space. It is driven by two base joint actuators. Then, the dimensions of $\boldsymbol{\tau}$, $\boldsymbol{k_u}$, and $[A]$ will be given as 2×1, 3×1, and 2×3, respectively. This implies that in order to modulate three independent stiffness elements in the operational space, only two joint actuators is employed in former operational-based compliance control scheme[13]. Fig. 2 tells how this algorithm in Eq. (4) works. The first figure in Fig. 2 shows that $\boldsymbol{\tau}$ is uniquely decided for the given $\boldsymbol{k_u}$, though there exist infinite sets of $\boldsymbol{k_u}$ to obtain a $\boldsymbol{\tau}$ vector. However, once the $\boldsymbol{\tau}$ vector is applied to the joint actuators, we cannot guarantee that $\boldsymbol{\tau}$ creates the same $\boldsymbol{k_u}$ in the operational space, as shown in the second figure in Fig. 2. This represents the inherent problem occurring in former operational-based compliance control scheme. It is remarked that this analysis is different from that in the previous work regarding independent joint-based compliance control scheme [12, 13]. Thus, in order to obviate such a problem, the number of inputs should be equal or greater than the number of independent stiffness elements of the operational stiffness matrix. In the previous works[12, 14], kinematically redundant manipulators were proposed to satisfy this requirement. However, for those systems, the number of joints increases as many as the number of degree of the operational space. For example,

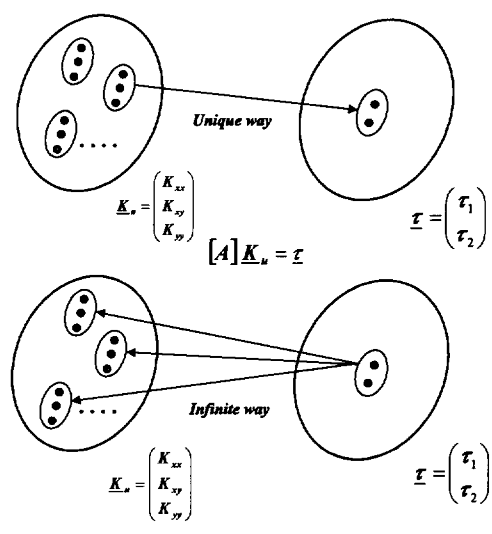

Fig. 2 : Mapping relation between $\boldsymbol{k_u}$ and $\boldsymbol{\tau}$.

to control 3 degree-of-freedom in the planar operational space, at least six joints are required to control six independent compliance elements for a 3x3 compliance matrix required in the operational space. To control 6 degree-of-freedom in the operational space, 21 joints are necessary. Too many joints and links may not be appropriate in the design aspect. Also, the inverse kinematic problem becomes complex as in the works of redundant manipulator[11,14]. Therefore, in this paper we propose an alternative approach for independent joint-based compliance control via redundant actuation.. The main idea is the utilization of redundant actuators which is in general the reality of biomechanical systems including the human body. For example, the human upper-extremity possesses 29 muscles which is enough to control 21 independent compliance elements of the 6x6 operational compliance matrix. However, the human upper extremity does not possess 21 joints, but instead, it has 7 joints and several closed-chain structures in which many muscles attached in different points. Conclusively, it is kinematically-redundant as little as possible, but is redundantly actuated as much as possible. The kinematic structure of the human upper extremity tells us how to design the manipulator for successful implementation of independent joint-based compliance control scheme. In this paper, we propose the independent joint-based compliance control by utilization of redundant actuators. A five-bar finger has been designed for experiment, and will be employed to verify the control algorithm proposed in this work.

3. Kinematic Modeling of Five-bar Finger

The modeling methodology integrates the *Generalized Principle of d'Alembert* with the method of kinematic influence coefficients(*KIC*) resulting in closed form vector expressions. The reader is referred to Freeman and Tesar [16] for a more detailed description of the following scheme. In the following, the letter G stands for *1st* order *KIC* matrix, and superscribed quantities are considered and indicate dependent parameters with subscripts denoting independent parameters.

3.1 Open-chain kinematics

Consider a 5-bar finger mechanism shown in Fig. 1. This system has one closed-kinematic chain. The closed-kinematic chain is formed by connecting the two open-chains at the given location of the second link of the left open-chain, as shown in Fig. 1. In order to enlarge the area encompassed by the finger, the folded-in configuration of the right open-chain is chosen. Since two n-chain of the 5-bar mechanism have a common kinematic relation at the end-point of the system, the components of the end-point vector $\boldsymbol{u}$ are described by

$$x = l_1 c_1 + l_2 c_{12} = l_3 c_3 + l_4 c_{34} + l_5 c_{345}, \qquad (5)$$

$$y = l_1 s_1 + l_2 s_{12} = l_3 s_3 + l_4 s_{34} + l_5 s_{345}, \qquad (6)$$

and

$$\Phi = \theta_1 + \theta_2 = \theta_3 + \theta_4 + \theta_5. \qquad (7)$$

Adopting the standard Jacobian representation for the velocity of a vector of N dependent (output) parameters $\boldsymbol{u}$ in terms of a set of P independent input coordinates ${}_r\dot{\boldsymbol{\phi}}$ of r^{th} open-chain, one has

$$\dot{\boldsymbol{u}} = [\,{}_rG^u_\phi\,]\ {}_r\dot{\boldsymbol{\phi}}_a. \qquad (8)$$

Here,

$$[\,{}_rG^u_\phi\,] = [\,\frac{\partial u}{\partial_r\phi_1}, \frac{\partial u}{\partial_r\phi_2}, \cdots, \frac{\partial u}{\partial_r\phi_P}\,] \qquad (9)$$

is the Jacobian relating the coordinates $\boldsymbol{u}$ to ${}_r\dot{\boldsymbol{\phi}}$, and is of dimension of $N\times P$, with the m^{th} column being of dimension of $N\times 1$. Jacobians of the first and second open-chain, respectively, are given by

$$[\,{}_1G^u_\theta] = \begin{bmatrix} -(l_1 s_1 + l_2 s_{12}) & -(l_2 s_{12}) \\ (l_1 c_1 + l_2 c_{12}) & (l_2 c_{12}) \\ 1 & 1 \end{bmatrix}, \qquad (10)$$

and

$$[\,{}_2G^u_\theta] = \begin{bmatrix} -l_3 s_3 - l_4 s_{34} - l_5 s_{345} & -l_4 s_{34} - l_5 s_{345} & -l_5 s_{345} \\ l_3 c_3 + l_4 c_{34} + l_5 c_{345} & l_4 c_{34} + l_5 c_{345} & l_5 c_{345} \\ 1 & 1 & 1 \end{bmatrix} \qquad (11)$$

3.2 Internal kinematics for 5-bar Finger mechanism

Since the mobility of this mechanism is two, at least two actuators are required to control the mechanism. There exist several choices in the selection of independent joints (i.e., actuator locations). In general, the base joints have been chosen as the actuator locations in previously developed 5-bar systems, primarily to minimize the dynamic effect due to floating actuators. However, from a kinematic point of view, inclusion of one or two floating actuators may be promising. For example, a better manipulability, isotropy, or load handling capacity can be achieved by using a certain floating actuator[19]. An internal kinematic relationship between dependent joints and independent joints is required to deal with the problem addressed in the above.

The equivalent velocity relation is given by

$$\dot{\boldsymbol{u}} = [\,{}_1G^u_\theta]\,{}_1\dot{\theta} = [\,{}_2G^u_\theta]\,{}_2\dot{\theta}. \qquad (12)$$

Choosing the joints θ_1 and θ_3 as the independent joints($\boldsymbol{\theta}_a$) and the joints θ_2, θ_4, and θ_5 as the dependent joints ($\boldsymbol{\theta}_p$), Eq. (12) can be rearranged according to the following form ;

$$[A]\,\dot{\boldsymbol{\theta}}_p = [B]\,\dot{\boldsymbol{\theta}}_a, \qquad (13)$$

where

$$[A] = [\,-[\,{}_1G^u_\theta]_{;2}\ [\,{}_2G^u_\theta]_{;2,3}\,], \qquad (14)$$

$$[B] = [\,[\,{}_1G^u_\theta]_{;1}\ -[\,{}_2G^u_\theta]_{;1}\,], \qquad (15)$$

$$\dot{\boldsymbol{\theta}}_p = (\ \dot{\theta}_3\ \ \dot{\theta}_4\ \ \dot{\theta}_5)^T, \tag{16}$$

and

$$\dot{\boldsymbol{\theta}}_a = (\ \dot{\theta}_1\ \dot{\theta}_2)^T. \tag{17}$$

Now, premultiplying the inverse of the matrix [A] to both sides of Eq. (13) yields[17]

$$\dot{\boldsymbol{\theta}}_p = [G_a^p]\ \dot{\boldsymbol{\theta}}_a, \tag{18}$$

where $[G_a^p]$ denotes the first-order *KIC* matrix relating $\boldsymbol{\theta}_p$ to $\boldsymbol{\theta}_a$.

According to the duality existing between the velocity vector and force vector, the force relation between the independent joints and the dependent joints is described by

$$\boldsymbol{T}_a = [G_a^p]^T \boldsymbol{T}_p. \tag{19}$$

Then, the effective load referenced to the independent joints is given by

$$\boldsymbol{T}_a^* = \boldsymbol{T}_a + [G_a^p]^T \boldsymbol{T}_p = [G_a^\phi]^T \boldsymbol{T}_\phi, \tag{20}$$

where

$$[G_a^\phi] = \begin{bmatrix} I \\ \\ [G_a^p] \end{bmatrix}, \tag{21}$$

$$\boldsymbol{T}_a = (\ T_1\ T_2)^T. \tag{22}$$

In Eq. (20), $\boldsymbol{T}_\phi$ denotes a force vector consisting of $\boldsymbol{T}_a$ and the whole set or subset of the joint torque at the dependent joints.

3.3 Forward Kinematics for 5-bar mechanism

Since the joints(${}_r\boldsymbol{\phi}$) of the r^{th} chain is composed of some of the independent and dependent joints, ${}_r\dot{\boldsymbol{\phi}}$ can be expressed in terms of the independent joints by

$${}_r\dot{\boldsymbol{\phi}} = [\ {}^rG_a^\phi]\ \dot{\boldsymbol{\phi}}_a, \tag{23}$$

where the matrix $[\ {}^rG_a^\phi]$ is formed by using elements of $[\ G_a^p]$ augmented with a unity in the i^{th} row and j^{th} column and with zeros in all other elements of the i^{th} row, if ${}_r\phi_i = \phi_{a_j}$. Thus, the forward kinematics for the common object is obtained by embedding the first-order internal KIC (Jacobian) into one of the r^{th} pseudo open-chain kinematic expressions as follows :

$$\dot{\boldsymbol{u}} = [\ {}_rG_\phi^u]\ {}_r\dot{\boldsymbol{\phi}} = [\ G_a^u]\ \dot{\boldsymbol{\phi}}_a, \tag{24}$$

where the forward Jacobian is determined by

$$[G_a^u] = [\ {}_rG_\phi^u][\ {}^rG_a^\phi]. \tag{25}$$

According to the duality existing between the velocity vector and force vector, the force relation between the independent joints and the dependent joints is described by

$$\boldsymbol{T}_a = [G_a^u]^T \boldsymbol{T}_u \tag{26}$$

and the inverse is given by

$$\boldsymbol{T}_u = [G_u^a]^T \boldsymbol{T}_a. \tag{27}$$

Now, the force relationship between $\boldsymbol{T}_u$ and $\boldsymbol{T}_\phi$ is given by

$$\boldsymbol{T}_u = [G_u^\phi]^T \boldsymbol{T}_\phi, \tag{28}$$

where

$$[G_u^\phi] = [G_a^\phi][G_u^a]. \tag{29}$$

4. Stiffness Modeling of Five-bar Finger

To perform a compliance control for five-bar finger, we employ an equivalent stiffness matrix instead of compliance matrix. We have placed four actuators in the five-bar finger. When we employ redundant joint actuators, the mapping relation from the input to output is not unique. Thus, we employ the inverse relation which is uniquely defined by

$$[G_u^\phi] = \begin{bmatrix} a_1 & b_1 \\ a_2 & b_2 \\ a_3 & b_3 \\ a_4 & b_4 \end{bmatrix}, \tag{30}$$

and the joint space stiffness matrix $[K_{\phi\phi}]$ and the operational space stiffness matrix $[K_{uu}]$ are given as

$$[K_{\phi\phi}] = \begin{bmatrix} k_{\phi 1} & 0 & 0 & 0 \\ 0 & k_{\phi 2} & 0 & 0 \\ 0 & 0 & k_{\phi 3} & 0 \\ 0 & 0 & 0 & k_{\phi 4} \end{bmatrix}, \tag{31}$$

and

$$[K_{uu}] = \begin{bmatrix} k_{xx} & k_{xy} \\ k_{yx} & k_{yy} \end{bmatrix}. \tag{32}$$

In a state of static equilibrium, Eq. (28) can be described as

$$\boldsymbol{T}_u = [G_u^\phi]^T \boldsymbol{T}_\phi = 0. \tag{33}$$

Given a disturbance to the system under force equilibrium, a spring-like behaviour occurs to the system. The total effective stiffness matrix $[K_{aa}]$ with respect to the independent coordinates is obtained by differentiating Eq. (33) with respect to the independent coordinate set $\boldsymbol{\phi}_a$ [17]

$$[K_{uu}] = [G_u^\phi]^T [K_{\phi\phi}][G_u^\phi] - T_\phi^T \circ [H_{uu}^\phi], \tag{34}$$

where the (i, j) element of k^{th} plane of the second-order influence coefficient matrix $[H_{uu}^\phi]$ is defined as [17]

$$[H_{uu}^{\phi_k}]_{(k,i,j)} = \frac{\partial}{\partial u_j}\left(\frac{\partial \phi_k}{\partial u_i}\right), \tag{35}$$

and the (i, j) element of Eq. (34) can be expressed as $\{(-\boldsymbol{T}_\phi)^T \circ [H_{uu}^\phi]_{(*,i,j)}\}$.

Eq. (34) can be expressed in a vector form

$$\boldsymbol{K}_u = [A]\ \boldsymbol{K}_\phi, \tag{36}$$

where

$$[A] = \begin{bmatrix} a_1^2 & a_2^2 & a_3^2 & a_4^2 \\ a_1 b_1 & a_2 b_2 & a_3 b_3 & a_4 b_4 \\ b_1^2 & b_2^2 & b_3^2 & b_4^2 \end{bmatrix}, \qquad (37)$$

$$\boldsymbol{K}_u = [k_{xx} \ k_{xy} \ k_{yy}]^T, \qquad (38)$$

$$\boldsymbol{K}_\phi = [k_{\phi 1} k_{\phi 2} k_{\phi 3} k_{\phi 4}]^T, \qquad (39)$$

and the particular solution for $\boldsymbol{K}_\phi$ is expressed as

$$\boldsymbol{K}_\phi = W^{-1} A^T (A W^{-1} A^T)^{-1} \ \boldsymbol{K}_u, \qquad (40)$$

where W^{-1} denotes a weighting matrix. With consideration of homogeneous solution, there exist infinite solutions for $\boldsymbol{K}_\phi$.

5. Experimental Works

Fig. 3 represents the prototype of the five-bar finger. Four actuators are placed to 1345 joints. Each joint of the finger is driven by a compact actuator mechanism having ultrasonic motor and a gear set with potentiometer, and the system is controlled by VME Bus-based Control system. The ultra-sonic motors have high torque/size ratio as compared to DC motor with a similar size. A gear transmission having about 15:1 speed reduction ratio is employed. Particularly, the gear transmission consisting of

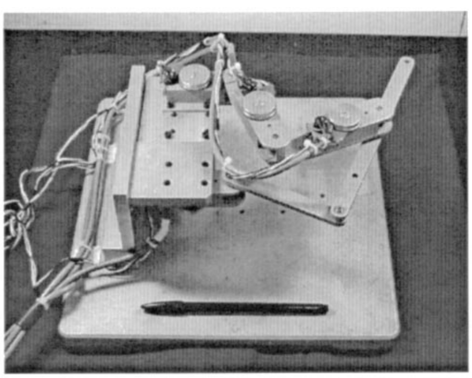

Fig. 3 : Prototype of Five-bar Finger

series of spur gears and the potentiometer are embedded inside the link, which yields compact and modular design of the finger mechanism. We have performed kinematic optimal design for this mechanism and have developed several internal force control algorithms in previous works [19-21].

A hybrid control is performed in our experiment. We control the position along the x-direction and the force along the y direction. A wall is placed parallel to the x-direction. The surface of the wall is very smooth, and thus the friction force is negligible when the finger tip moves along the wall surface. The force controlled in the vertical direction will be planned by

$$F_y = K_{yy} \Delta y. \qquad (41)$$

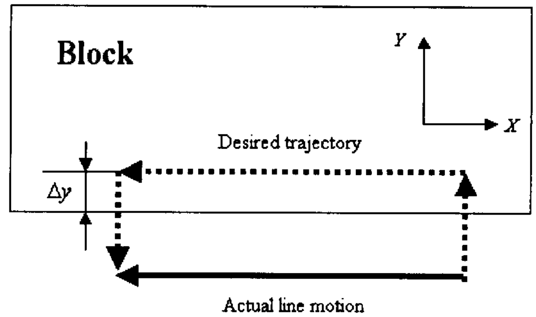

Fig. 4 : Trajectory for Hybrid Control

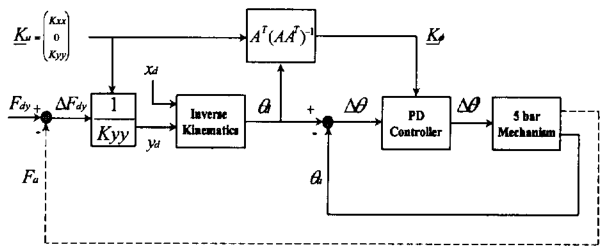

Fig. 5 : Block Diagram for Hybrid Control

In this experiment, we choose the operational space stiffness along the y-direction relatively compliant when compared with that in the x-direction. Fig. 4 shows the trajectory of our hybrid control experiment, and Fig. 5 describes the block diagram for hybrid control of five-bar finger with redundant actuation.

In a finger manipulation, measuring the finger-tip force has become a bottle neck, though there are a few suggestions [23, 24] to resolve this problem. In our experiment, we measure the finger-tip force by placing a force/torque sensor on the back of the wall. The stiffness along the y-direction is 500 N/m, and 3 N of force is controlled by inducing a displacement Δy of 6 mm inside the wall.

Two experiments have been performed ; The first one only considers the first-term of Eq. (34), and the second one considers the both terms of Eq. (34). Initially, Yi, et.al.[17] performed a detailed analysis for the additional term $T_\phi^T \circ [H_{uu}^\phi]$. Choi, et.al[14] and Howard and Kumar [22] also modeled this additional term made by the change of the system configuration. As shown in Fig. 6 and Fig. 7, the effect of $T_\phi^T \circ [H_{uu}^\phi]$ cannot be negligible. Fig. 8 represents the magnitudes of the stiffness elements for $T_\phi^T \circ [H_{uu}^\phi]$ calculated along the trajectory. The effect will be much significant as the magnitude of controlled-force increases and also the system moves to a configuration where the Frobenius norm of $[H_{uu}^\phi]$ becomes large. Fig. 9 also shows the position history along the planned trajectory.

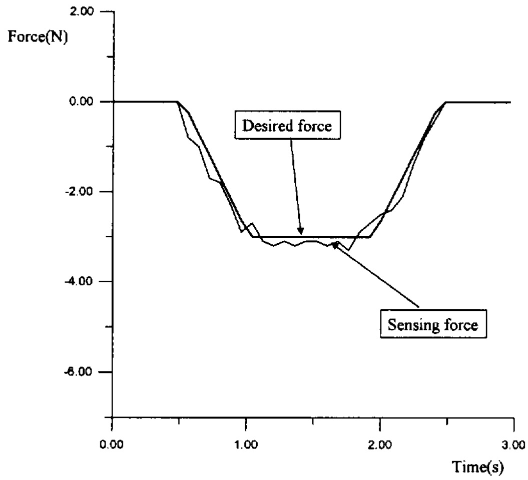

Fig. 6 : Force Control(Experimental Result Without Consideration of $T_\phi^T \circ [H_{uu}^\phi]$)

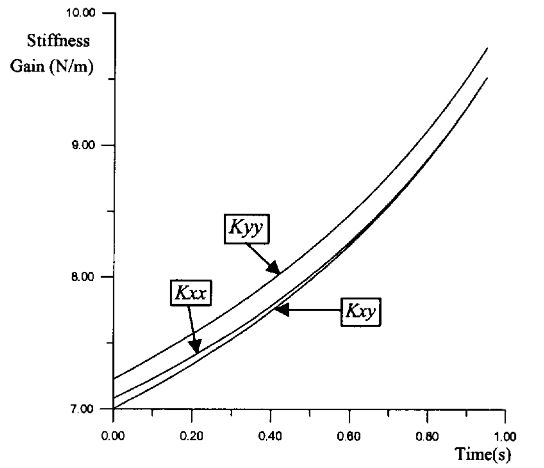

Fig. 8 : Stiffness Elements for $T_\phi^T \circ [H_{uu}^\phi]$ Along the Trajectory

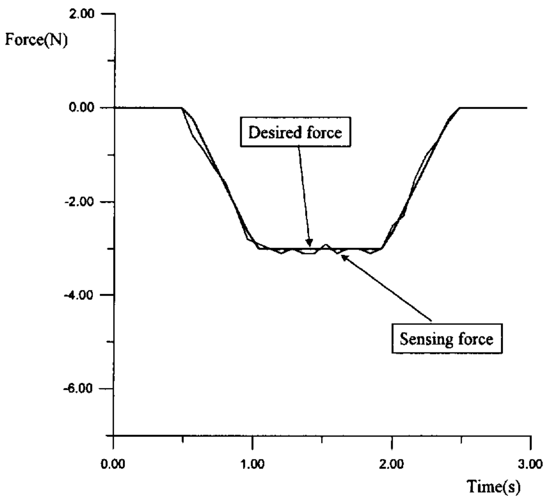

Fig. 7 : Force Control(Experimental Result With Consideration of $T_\phi^T \circ [H_{uu}^\phi]$)

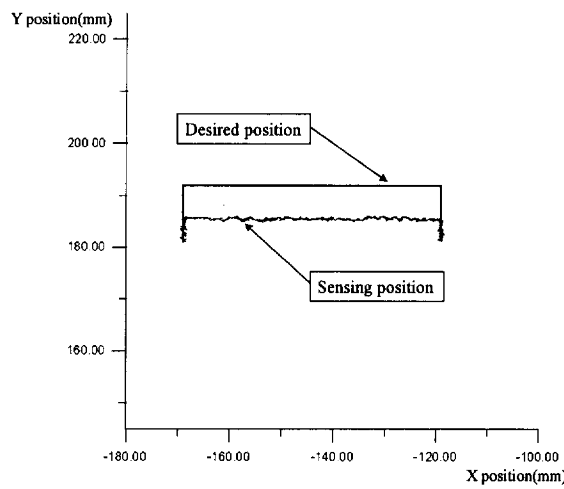

Fig. 9 : Experimental Result for Hybrid Control Scheme with Redundant Actuation

So far we demonstrated our successful experimental result for independent joint-based compliance control scheme. In order to compare our result with the performance of former compliance control method, we performed experimental work for the former compliance control scheme. However, as discussed in section 2, we could not obtain any successful experimental results.

Conclusively, the former compliance control scheme has two shortcomings in comparison to the proposed compliance control scheme. First, it cannot guarantee the successful result in compliance control. Secondly, it does not have any other alternative in both algorithm development and control commands since there are no force redundancies. On the other hand, redundant actuators enables the system to generate larger payload and to perform several subtasks.

In our experiments, we performed an open-loop force control without feedback of the measured force data from F/T sensor. As one of the future work, we will consider a closed-loop force control by inserting a force sensor into an appropriate location of the system[23] or by estimating the force by disturbance observer[24].

6. Conclusions

In this paper, we proposed a joint-based compliance control scheme. We explained, in our point of view, why the former operational-based compliance control scheme is not appropriate, which naturally introduces the necessity of independent joint-based compliance control scheme. Also, we addressed types of robot structures which are much appropriate to independent joint-based compliance scheme through explanation of nature of the human body, which typically possess force redundancy as well as kinematic redundancy, which enables one to modulate the operational stiffness in a more adequate way. As an illustrative example, we investigated a five-bar finger mechanism which has two redundant actuators in its structure. Our experimental results showed that former compliance control schemes did not always guarantee modulation of the required operational compliance matrix, while the compliance modulation of the proposed method could be satisfactory. We also considered an additional stiffness effect due to the antagonistic fighting between the controlled-operational force and the equilibriumed joint torque vector. It was experimentally shown that consideration of this additional term notably improved the force tracking performance of the given mechanism.

The extension of this work to control of multi-fingered hands will be a natural process. We plan to apply the independent joint-based compliance control scheme to control of dual five-bar finger system which will be used for grasping an object and manipulating it for various applications.

Acknowledgement

The work has been supported by KIST 2000 Human Robot project.

References

[1] Nakamura, Y. and Ghodoussi, M., Dynamic computation of closed-link robot mechanisms with nonredundant and redundant actuators. *IEEE Journal of Robotics and Automation,* Vol. 5, pp. 294-302, 1989.

[2] Nahon, M.A. and Angeles, J., Force optimization in redundantly-actuated closed kinematic chains. *IEEE Proceeding on Robotics and Automation Conference*, pp. 951-956, 1989.

[3] Kumar, V.J. and Gardner, J., Kinematics of redundantly actuated closed chain. *IEEE Journal of Robotics and Automation,* Vol. 6, pp. 269-273, 1990.

[4] Kurz, R. and Hayward, W., Multiple-goal kinematic optimization of a parallel spherical mechanism with actuator redundancy. *IEEE Journal of Robotics and Automation,* Vol. 8, pp. 644-651, 1992.

[5] Mason, M.T., "Compliant Motion - Robot Motion," - in Brady, M. et.al. eds., *M.I.T Press*, 1983.

[6] Salisbury, J.K., "Active Stiffness Control of a Manipulator in Cartesian Coordinates," *IEEE Int. Conf. on Decision and Control*, 1980.

[7] Colbaugh, R. and Engelmann, A., "Adaptive Compliant Motion Control of Manipulators Theory and Experiments", *IEEE Int. Conf. on Robotics and Automation*, pp. 2719-2726, 1994.

[8] De Schutter, J., "A Study of Active Compliant Motion Control Methods for Rigid Manipulators Based on A Generic Scheme,"*IEEE Int. Conf. on Robotics and Automation*, pp. 1060-1065, 1987.

[9] Kazerooni, H. and Guo, J., "Direct-Drive, Active Compliant End-Effector," *IEEE Int. Conf. on Robotics and Automation*, pp. 758-766, 1987.

[10] Kato, A., Kondo, N., Narita, H., Ito, K., and Luo, Z.W., "Compliance Control of Direct Drive Manipulator Using Ultrasonic Motor", *Proc. of RoMan.* 1994.

[11] Mussa-Ivaldi, et.al., "Integrable Solutions of Kinematic Redundancy via Impedance Control," *J. of Robotics Research*, Vol. 10, No. 5, pp. 481-491, 1991.

[12] Yokoi, K., Maekawa, H., and Tanie, K, "A Method of Compliance Control for a Redundant Manipulator," *IEEE/RSJ Conf. on Intelligent Robots and Systems*, pp. 1927-1934, 1992.

[13] Yokoi, K., Kaneko, H., and Tanie, K, "A Compliant Control Method Suggested by Muscle Networks in Human Arms," *IEEE/RSJ Int. Conf. on Intelligent Robots and Systems*, pp. 385-390, 1988.

[14] Choi, H.R., Chung, W.K., and Youm, Y., "Stiffness Analysis and Control of Redundant Manipulators", *IEEE Int. Conf. on Robotics and Automation*, pp. 689-695, 1994.

[15] Tao, J.M., Luh, J.S., and Zheng, Y.F., "Compliant Coordination Control of Two Moving Industrial Robots", *IEEE J. of Robotics and Automation*, pp. 322-330, 1990.

[16] Freeman, R.A. and Tesar, D., "Dynamic Modeling of Serial and Parallel Mechanisms/Robotic Systems, Part I-Methodology, Part II-Applications," *Proc. 20th ASME Biennial Mechanisms Conf. Orlando, FL, Trends and Development in Mechanisms, Machines, and Robotics,* DE-Vol.15-3, pp.7-27, 1988.

[17]Yi, B-J. et.al., "Geometric Stability in Force Control," *IEEE Int. Conf. on Robotics and Automation*, pp. 281-286, 1991.

[18 Yi, B-J. and Freeman, R.A., "Geometric Analysis of Antagonistic Stiffness in Redundantly Actuated Parallel Mechanisms," *Journal of Robotic Systems* Vol. 10, pp. 581-603, 1993.

[19] Yi, B-J., Suh, I.H., and Oh, S-R., "Analysis of a five-bar finger mechanism having redundant actuators with applications to stiffness and frequency modulation," *IEEE Proceeding on Robotics and Automation Conference*, pp. 759-765, 1997.

[20] Yi, B-J., Oh, S-R., and Suh, I.H., "Synthesis of actively adjustable frequency modulators : The case for a five-bar finger mechanism,". *IEEE/RSJ Proceeding on Intelligent Robot and Systems,* pp. 1098-1104, 1997.

[21] Lee, J.H., Yi, B-J., Oh, S-R., and Suh, I.H., "Optimal Design of a Five-bar Finger with Redundant Actuation," *IEEE Proceeding on Robotics and Automation Conference*, pp. 2068-2074, 1998.

[22] Howard, W.S. and Kumar, V.J., "Modeling and Analysis of the Compliance and Stability of Enveloping Grasps," *IEEE Proceeding on Robotics and Automation Conference*, pp. 1367-1372, 1995.

[23] Kaneko, K, Yokoi, K., and Tanie, K., "On a New Torque Sensor for Tendon Drive Fingers," *Trans. on Robotics and Automation*, Vol. 6, No. 4, pp. 501-510, 1990.

[24] Eom, K.S., Suh, I.H., Chung, W.K., and Oh, S.-R., "Disturbance Observer Based Force Control of Robot Manipulator Without Force Sensor," *IEEE Proceeding on Robotics and Automation Conference*, pp. 3012-3017, 1998.